ELSEVIER

Physica B 259–261 (1999) 576–581

PHYSICA B

Rare earth magnetic order in RNi_2B_2C and RNiBC

S. Skanthakumar[a,*], J.W. Lynn[b]

[a]*Chemistry Division, Argonne National Laboratory, Argonne, IL 60439, USA*
[b]*NIST Center for Neutron Research, NIST, Gaithersburg, MD 20899, USA*

Abstract

A review of neutron diffraction experiments on the magnetic order in the RNi_2B_2C and RNiBC (R – rare earth) systems is given. The RNi_2B_2C materials exhibit a wide variety of commensurate and incommensurate magnetic structures for different rare earths, along with superconductivity that is coupled to the magnetism. Simple commensurate antiferromagnetic structures are observed for R = Pr ($T_N = 4.0$ K), Nd ($T_N = 4.8$ K), Ho ($T_N = 8.5$ K) and Dy ($T_N = 11$ K). In addition, $HoNi_2B_2C$ exhibits a *c*-axis spiral and an *a*-axis modulated incommensurate structure above 5 K, while both structures collapse in favor of the commensurate structure at low T. A transversely polarized spin density wave (SDW) type incommensurate structure is observed for Er ($T_N = 6.8$ K) and Tm ($T_N = 1.5$ K), while a longitudinally polarized SDW structure is observed for Tb ($T_N = 15$ K). No magnetic ordering of any type is detected for Y, Ce and Yb. HoNiBC is an antiferromagnet ($T_N = 9.8$ K), ErNiBC is ferromagnetic ($T_C = 4.6$ K), while TbNiBC and DyNiBC exhibit both ferromagnetic and antiferromagnetic ordering at 17 K and ~ 12 K, respectively. Published by Elsevier Science B.V. All rights reserved.

Keywords: Magnetic structure; Neutron diffraction; Magnetic transitions; Borocarbides

The magnetic ordering in superconducting systems has attracted considerable interest, both because of the intrinsic interest in magnetism and because of the possibility to study the interplay between long-range magnetic order and superconductivity (for a recent review see Ref. [1]). In general, rare earth magnetic ordering temperatures (T_N) are lower than the superconducting temperatures (T_C), while for RNi_2B_2C T_N and T_C are comparable, and thus the magnetic and superconducting condensation energies are also comparable. Hence the interplay between superconductivity and magnetic order is expected to be strong in this system, and has been studied in great detail [2–7]. In this paper we present a summary of the results that we have obtained from our neutron diffraction experiments at the NIST Center for Neutron Research, which were conducted to study the magnetic ordering of rare-earth ions in RNi_2B_2C and RNiBC. A wide variety of spin structures, such as simple commensurate antiferromagnet, transverse spin density wave, longitudinal spin density wave and spiral, is observed in these materials. Experimental details can be found elsewhere [2].

Room temperature structural refinements showed that most of the RNi_2B_2C samples were single phase. All the nuclear peaks can be indexed as (h, k, l) with $h + k + l =$ even, and our analysis indicates that RNi_2B_2C crystallizes in the body-centered-tetragonal I4/mmm space group in agreement with the original analysis [8]. In RNi_2B_2C, R–C layers alternate along the *c*-axis with Ni_2B_2 layers. Magnetic ordering in this system arises from the rare earth ions, and there are two rare earth ions in a unit cell: one is at the origin and the other is at the body centered position. No ordered magnetic moment was detected on the Ni site. Both the lattice parameter *a* and the volume of the unit cell decrease with decreasing rare earth ionic radius while the lattice parameter *c* increases. This behavior, which is also observed with decreasing temperature, arises due to the strong Ni–B and B–C bonding [2].

*Corresponding author. Fax: 630 252 4225; e-mail: skantha@anl.gov.

0921-4526/99/$ – see front matter
PII: S0921-4526(98)00730-3

In order to get information about the magnetic ordering, we have used the subtraction technique, where we collect data above the ordering temperature (T_N) and subtract from the data obtained below T_N. If there is no significant change in the nuclear structure then the magnetic diffraction pattern is obtained. To demonstrate this, we show the neutron powder diffraction data collected on $TbNi_2B_2C$, where the Tb ordering temperature is 15 K, in Fig. 1. Above the transition temperature (20 K), we observe only nuclear Bragg peaks as shown in Fig. 1b. Below the transition temperature (4.5 K), additional magnetic Bragg peaks develop as indicated by the arrows in Fig. 1a. Once we subtract the 20 K data from 4.5 K, the nuclear peaks cancel and only magnetic peaks survive as shown in Fig. 1c. Information about the magnetic ordering, such as spin structure, spin direction, nature of magnetic order, can be obtained by using the positions, widths, relative intensities, and temperature dependence of these magnetic Bragg peaks. Since the magnetic intensities are proportional to the square of the magnetic moment, the absolute ordered magnetic moment of the rare earth ion can be obtained by comparing the magnetic Bragg peak intensities to those of nuclear Bragg peaks.

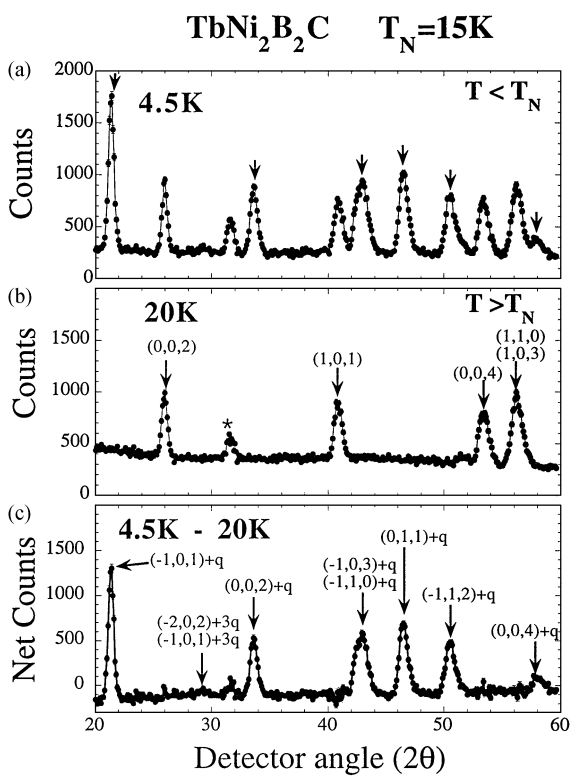

Fig. 1. Neutron diffraction pattern for $TbNi_2B_2C$, which has T_N of 15 K. (a) At 4.5 K, which is below T_N, both nuclear and magnetic peaks are observed. Arrows indicate the magnetic peaks; (b) data at 20 K (above T_N) where only nuclear peaks are observed. * indicates an impurity peak. (c) Magnetic diffraction pattern obtained by subtracting the 20 K data from the data at 4.5 K.

We have studied Y, Ce, Pr, Nd, Tb, Dy, Ho, Er, Tm and Yb using neutron diffraction techniques. Information about Gd and Sm, which are highly neutron absorbing elements, were obtained from X-ray experiments by Detlefs et al. [9,10], and we include this information here for completeness. No magnetic ordering is observed in superconducting ($T_C = 15.5$ K) YNi_2B_2C, or in $CeNi_2B_2C$ and $YbNi_2B_2C$. X-ray absorption and lattice parameter measurements in $CeNi_2B_2C$ indicate that Ce has a mixed-valent state in this system [11], and this could explain the absence of superconductivity. Moderate heavy fermion behavior is observed for Yb in $YbNi_2B_2C$, and the suppression of superconductivity may be due to strong hybridization between the conduction electrons and the 4f states [12–14].

A simple commensurate antiferromagnetic structure is observed for Pr, Dy and Ho (< 5 K) ions in RNi_2B_2C [2]. The observed magnetic peaks in these compounds can be indexed as (h, k, l) with $h + k + l =$ odd based on the chemical unit cell, and therefore the magnetic and chemical unit cells are the same. The magnetic structure is shown in Fig. 2a, where we see that the moments form ferromagnetic sheets in the a–b plane, and these sheets are coupled antiferromagnetically along the c-axis, with the spin direction in the a–b plane. However, the easy direction within this plane cannot be obtained by (zero field) neutron diffraction data, which average over all possible domains. The temperature dependence of the (0,0,1) Pr magnetic Bragg peak, which is shown in Fig. 3a, indicates that the ordering temperature is 4.0(1) K. The ordered moment for Pr is observed to be $0.81(3)\mu_B$ at 1.5 K and no superconductivity is observed in $PrNi_2B_2C$. $DyNi_2B_2C$, which superconducts at 6 K, has the same spin structure as Pr, with the easy direction along (1, 1, 0) determined from magnetization measurements [15]. The magnetic ordering temperature in $DyNi_2B_2C$ is ~ 11 K, and the ordered moment is $8.47(9)\mu_B$. Recently, large hysteresis and reentrant behavior has been observed at low temperatures in this compound [16], and more work is needed to obtain a complete understanding of this behavior.

$HoNi_2B_2C$, which is found to be a very interesting compound in this system, starts to superconduct at about 8 K, then returns to the normal state briefly at 5 K, and finally reenters the superconducting state again with further decrease of the temperature [17]. This behavior is closely connected to the magnetic ordering behavior in this system [3,4]. Below the ordering temperature of 8.5 K, two types of structures develop. One is a commensurate antiferromagnetic structure, which is similar to the one observed for Pr and Dy compounds (Fig. 1a). The other is a c-axis spiral incommensurate structure,

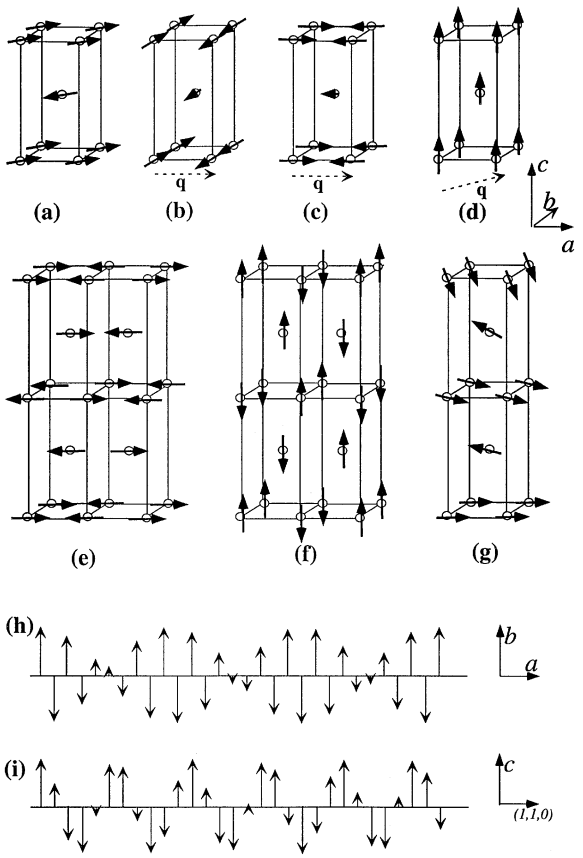

Fig. 2. Observed magnetic structures for the rare earth ions in RNi_2B_2C. (a) Simple antiferromagnetic structure of Pr, Dy and Ho. Spins are in the a–b plane. (b) Transverse spin density wave of Er and Gd, where spins are along b. (c) Longitudinal spin density wave of Tb, where spins are along a (d) Transverse spin density wave of Tm, where the spins point along c. (e) Nd commensurate magnetic structure (f) Sm commensurate magnetic structure (g) Spiral magnetic structure of Ho, which is observed between 5 and 8 K. Transversely polarized spin density wave structures of (h) Er with modulation along a-axis and (i) Tm with modulation along (1, 1, 0)-axis, which are shown over several unit cells. Gd and Sm magnetic order information is obtained from X-ray measurements. [9,10].

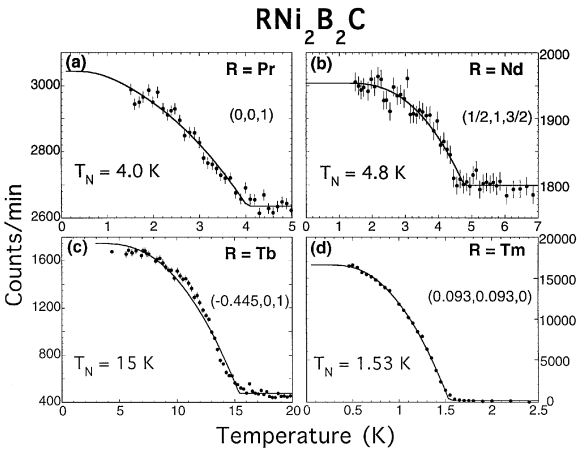

Fig. 3. Temperature dependence of the intensities of magnetic Bragg peaks of (a) Pr, (b) Nd, (c) Tb and (d)Tm, which show magnetic transition temperatures of 4.0, 4.8, 15 and 1.53 K, respectively. The solid curves are fits to a Brillouin function.

which is shown in Fig. 1g, with a modulation vector of (0, 0, 0.91). This structure contains ferromagnetic layers in the a–b plane as in the commensurate structure, but adjacent layers along the c-axis have a relative alignment of $\sim 163.4^\circ$ instead of 180°. Below 6.5 K, another incommensurate structure develops with an a-axis modulation (0.55, 0, 0). Since only weak intensities were observed from this structure, the detailed spin structure has not been determined yet. Below 5 K, where the superconductivity is reentrant, both incommensurate structures lock into the commensurate antiferromagnetic one. This allows the superconductivity to return and coexist with the antiferromagnetism. The ordered moment is $8.62(6)\mu_B$, and magnetization measurements [15] indicate that the easy axis is along (1 1 0). Initially it was thought that the c-axis spiral structure is responsible for the reentrant behavior at 5 K, as this structure produces a net field on the Ni ions that are responsible for superconductivity [3]. However, recent measurements on $Ho_xY_{1-x}Ni_2B_2C$ indicate that the a-axis structure might be responsible for the reentrant behavior [7].

A different type of commensurate antiferromagnetic structure is observed for the non-superconducting Nd and Sm compounds. All the observed magnetic Bragg peaks can be indexed as $(h/2, k, l/2)$ based on the chemical unit cell, where h and l are odd integers and k is any integer. In this case the magnetic unit cell is double the chemical unit cell along the a and c directions while it is the same along b as shown in Fig. 2e and f. In $NdNi_2B_2C$, our analysis indicates that the Nd moment is along the a-axis as shown in Fig. 2e, and the ordered moment is $2.10(7)\mu_B$. The observed peak positions and indexing are given in Table 1 along with the observed and calculated intensities. The modulation vector $\boldsymbol{q}$ is $(\frac{1}{2}, 0, \frac{1}{2})$, with an equivalent domain where $\boldsymbol{q} = (0, \frac{1}{2}, \frac{1}{2})$ and moment direction is along b. The temperature dependence of the $(\frac{1}{2}, 1, \frac{3}{2})$ magnetic peak is shown in Fig. 3b, and indicates that T_N is 4.8 K. This spin structure is in agreement with the structure obtained by recent X-ray scattering measurements [9]. The Sm spin structure has also been investigated with X-rays and is similar to that of Nd, but with the magnetic moment along the c-axis as shown in Fig. 2f. The ordering temperature is 9.8 K, but the ordered moment has not yet been determined.

Spin density wave (SDW) type incommensurate magnetic structures are observed for the Er, Tb, Gd and Tm

Table 1
Observed and calculated intensities of the magnetic Bragg intensities in $NdNi_2B_2C$. These data were collected with an incident wavelength of 2.351 Å

Peak position (2θ) in deg.	Indexing	Obs. intensity	Cal. intensity
19.71	$(\frac{1}{2}, 0, \frac{1}{2})$	101 ± 22	107
27.57	$(\frac{1}{2}, 0, \frac{3}{2})$	257 ± 31	255
38.96	$(\frac{1}{2}, 0, \frac{5}{2})$	203 ± 31	181
42.54	$(\frac{1}{2}, 1, \frac{1}{2})$	339 ± 28	319
47.00	$(\frac{1}{2}, 1, \frac{3}{2})$	236 ± 27	273
51.96	$(\frac{1}{2}, 0, \frac{7}{2})$	224 ± 110	116
55.12	$(\frac{1}{2}, 1, \frac{5}{2})$	333 ± 100	210

Table 2
Observed and calculated intensities of the magnetic Bragg intensities in $TbNi_2B_2C$. These data were collected with an incident wavelength of 2.351 Å

Peak position (2θ) in deg.	Indexing	Obs. intensity	Cal. intensity
21.35	$(-1, 0, 1) + \boldsymbol{q}$	856 ± 18	786
29.06	$(-1, 0, 1) + 3\boldsymbol{q}$	97 ± 10	97
	$(-2, 0, 2) + 3\boldsymbol{q}$		
33.63	$(0, 0, 2) \pm \boldsymbol{q}$	479 ± 16	499
42.85	$(-1, 1, 0) + \boldsymbol{q}$	817 ± 22	835
	$(-1, 0, 3) + \boldsymbol{q}$		
46.51	$(0, 1, 1) \pm \boldsymbol{q}$	683 ± 18	655
50.56	$(-1, 1, 2) + \boldsymbol{q}$	546 ± 19	614
58.08	$(0, 0, 4) \pm \boldsymbol{q}$	191 ± 21	221

compounds. In superconducting $ErNi_2B_2C$ ($T_C = 11$ K), the Er spins starts to order at 6.8 K with a transversely polarized SDW type structure (i.e. with $\boldsymbol{q}$ and spin direction orthogonal). The spin structure is shown in Fig. 2b, where $\boldsymbol{q}$ is (0.5526, 0, 0) and the spin direction is along b. In order to demonstrate this structure more clearly, the spin density wave is shown over several unit cells along a in Fig. 2h. There are two different waves present. One is a short period of $\boldsymbol{q} = (0.5, 0, 0)$, which gives a simple commensurate antiferromagnetic structure. Therefore, most of the nearest-neighbor Er spins are aligned antiparallel along a. The second is a longer (~ 10 times larger than the first one) period with $\boldsymbol{q}$ of (0.0526, 0, 0), and this describes the modulation away from the commensurate structure. At low temperature a sinusoidal spin density wave cannot be the ground state, so the magnetic structure is expected to square-up (or to lock-in) and develop higher order harmonics. The observed amplitudes for sinusoidal moments are 9.15(12), 2.77(30) and 1.53(40)μ_B for μ_1, μ_3 and μ_5, respectively. This gives a low-temperature moment of 7.19(10)μ_B for Er [2]. We note that recent high-resolution X-ray diffraction experiments on single crystals of $ErNi_2B_2C$ indicate a tetragonal to orthorhombic structural transition near the magnetic ordering temperature, and the origin of this transition is attributed to magnetoelastic effects [18]. The resolution in our neutron powder data is not sufficient to detect such a small distortion.

The Gd ordering in non-superconducting $GdNi_2B_2C$ has been investigated using X-ray scattering experiments by Detlefs et al. [10] Gd orders at 19.4 K into a SDW with $\boldsymbol{q} = (0.55, 0, 0)$ and the spin direction is along b, i.e. initially Gd has the same structure as Er (Fig. 2b). However, below 13.6 K an additional ordered moment develops along the c-axis. Since Gd is a spin-only ion, there are no significant crystal-field effects and the ground state moment is expected to be 7 μ_B.

The Tb ions order with a modulation vector $\boldsymbol{q} = (0.555, 0, 0)$, which is similar to the one for Er, and the magnetic diffraction pattern is shown in Fig. 1c. The widths of the magnetic peaks are the same as those of the nuclear peaks, and this indicates that long range magnetic order has developed in this compound. These magnetic peaks can be indexed as $(h, k, l) + n\boldsymbol{q}$, with $h + k + l =$ even and $n = \pm 1$ or ± 3. The observed peak positions and indexing are given in Table 2 along with the observed and calculated intensities. Unlike the Er spin structure, though, the Tb spin structure is longitudinally polarized, where the modulation vector and moment direction are parallel, and this structure is shown in Fig. 2c. The observed amplitudes for the sinusoidal moments are 9.90(36) and 2.28(13)μ_B at 1.7 K for μ_1 and μ_3, respectively. This gives a low-temperature moment of 7.78(28)μ_B for Tb. The temperature dependence of the $(-1, 0, 1) + \boldsymbol{q}$ magnetic Bragg peak is shown in Fig. 3c, and this indicates the ordering temperature is about 15 K. Our observed modulation vector and the ordering temperature are in good agreement with measurements on single crystals [5]. In addition, a weak ferromagnetic component for Tb is also observed below 8 K in those measurements. It is very difficult to detect such a weak component from our powder data directly. However, our order parameter (Fig. 3c) shows a small anomaly around 10 K, and this might be due to the weak ferromagnetic component.

The Tm ions order with a modulation vector along (1, 1, 0) direction, which is different from other incommensurate structures. The observed magnetic peaks can be indexed as $(h, k, l) + n\boldsymbol{q}$, with $h + k + l =$ even, $\boldsymbol{q} = (0.093, 0.093, 0)$ and $n = \pm 1$ or ± 3. The observed peak positions and indexing are given in Table 3 along with the observed and calculated intensities. The Tm spin structure is a transversely polarized spin density wave, and this structure is shown in Fig. 2d. In order to demonstrate this structure clearly, the spin density wave is shown over several unit cells along (1, 1, 0) in Fig. 2i,

Table 3
Observed and calculated intensities of the magnetic Bragg intensities in $TmNi_2B_2C$. These data were collected with an incident wavelength of 2.351 Å

Peak position (2θ) in deg.	Indexing	Obs. intensity	Cal. intensity
5.09	$\boldsymbol{q}$	5392 ± 50	5455
38.07	$(-1, 0, 1) + \boldsymbol{q}$	365 ± 10	339
45.51	$(1, 0, 1) + \boldsymbol{q}$	261 ± 10	244
48.53	$(-1, -1, 2) + 3\boldsymbol{q}$	12 ± 5	12
51.18	$(-1, -1, 0) + \boldsymbol{q}$	75 ± 12	53
53.89	$(-1, 0, 3) + \boldsymbol{q}$	94 ± 16	87
57.58	$(-1, 1, 0) + \boldsymbol{q}$	127 ± 58	83
	$(-1, -1, 2) + \boldsymbol{q}$		
59.67	$(1, 0, 3) + \boldsymbol{q}$	180 ± 160	85

Table 4
Summary of magnetic transition temperature (T_n in K), modulation vector (δ), spin direction, magnetic structure (in Fig. 2) and ordered moment (μ in μ_B) for various R in RNi_2B_2C. ? indicates "unknown". Dy, Ho, Er, and Tm compounds superconduct with transition temperatures of 6, 8, 11 and 11 K, respectively. Information about Gd and Sm, which are highly neutron absorbing elements, were obtained from X-ray data. [9,10]. No magnetic ordering is observed in R = Y, Ce and Yb. Spin directions of Dy and Ho are obtained from magnetization measurements [15]

R	T_n	$\boldsymbol{q}$	Dir.	Str.	μ
Pr	4.0	(0, 0, 1)	*a–b*	*a*	0.81
Nd	4.8	(1/2, 0, 1/2)	*a*	*e*	2.10
Sm	9.8	(1/2, 0, 1/2)	*c*	*f*	?
Gd	19	(0.55, 0, 0)	*b*	*b*	?
	14	(0.55, 0, 0)	*b–c*	?	7
Tb	15	(0.555, 0, 0)	*a*	*c*	7.8
Dy	11	(0, 0, 1)	110	*a*	8.47
Ho	8.5	(0, 0, 0.91)	*a–b*	*g*	6.7
	6.3	(0.55, 0, 0)	?	?	?
	5	(0, 0, 1)	110	*a*	8.62
Er	6.8	(0.5526, 0, 0)	*b*	*b*	7.19
Tm	1.5	(0.093, 0.093, 0)	*c*	*d*	3.78

which is quite different from the one for Er (Fig. 2h). The observed amplitudes for sinusoidal moments are 4.81(18) and 0.93(19)μ_B at 0.36 K for μ_1 and μ_3, respectively. This gives a low-temperature moment of 3.78(14)μ_B for Tm. The temperature dependence of the magnetic Bragg peak is shown in Fig. 3d, and indicates an ordering temperature of ~ 1.5 K.

In Table 4, we give a summary of information about the rare earth magnetic ordering in RNi_2B_2C. Since the ordering temperature for dipole interactions is expected only to be ~ 1 K or less, the high-ordering temperatures in RNi_2B_2C show that magnetic interactions are dominated by exchange rather than dipole. Superconductivity and long-range magnetic order coexist in Dy, Ho, Er and Tm, and there is a clear evidence for the interaction between magnetic order and superconductivity in Ho. Both commensurate (Pr, Nd, Sm, Dy, Ho) and incommensurate spin structures (Gd, Tb, Ho at T > 5K, Er, Tm) are observed in this system. Modulation vectors for commensurate structures are either along *c*-axis (Pr, Dy, Ho) or along (1, 0, 1) direction (Nd, Sm). Modulation vectors for incommensurate structures are sometimes either along the *a* (Gd, Tb, Ho, Er) or *c* (Ho) axis and sometimes along (1, 1, 0) direction (Tm). The ordered moments for Sm and Tm are along the *c*-axis, while moments of all other ions are in the *a–b* plane, and this is determined mainly by crystal field anisotropy.

The wide variety of magnetic structures observed for the different rare earth ions strongly indicates that the Ruderman–Kittel–Kasuya–Yosida (RKKY)-type of exchange interaction plays an important role in stabilizing these magnetic structures. The magnetic structure is controlled by the conduction electron susceptibility, which varies from material to material, and hence different structures are stabilized for different rare earths. The calculation of the susceptibility for $LuNi_2B_2C$ showed a peak at $\boldsymbol{q} = (0.6, 0, 0)$, which is close to the modulation vectors observed for Gd, Tb, Ho and Er compounds [19]. Recently, the commensurate to incommensurate transition in $HoNi_2B_2C$ has also been interpreted in terms of the RKKY interaction, which competes with the crystalline electric field [20]. More theoretical work is needed to fully understand the magnetism and superconductivity in this system.

Finally, we discuss recent results of the related RNiBC system. RNiBC crystallizes in the tetragonal P4/nmm space group, and in this structure R_2C_2 bilayers alternate along the *c*-axis with Ni_2B_2 layers [8,21,22]. The Ho ions in HoNiBC order antiferromagnetically, with an ordering temperature of 9.8 K. In this compound, the magnetic unit cell is double the chemical unit cell along the *c* direction while it is the same along *a* and *b*. The Ho spins in each bilayer of Ho_2C_2 order ferromagnetically, and adjacent bilayers are coupled antiferromagnetically along the *c*-axis. The ordered moment, which is in the *a–b* plane, is 6.74(9)μ_B at 2.1 K [21]. ErNiBC is found to order ferromagnetically at $T_C = 4.6$ K [22,23], while TbNiBC and DyNiBC [23,24] exhibit both ferromagnetic and antiferromagnetic transitions at 17 K and 12 K, respectively.

We would like to thank our collaborators E. Baggio-Saitovitch, F. Bourdarot, R.J. Cava, C. Godart, T. Grigereit, L.C. Gupta, Z. Hossain, Q. Huang, J.J. Krajewski, R. Nagarajan, W.F. Peck, Jr., A. Santoro and S.K. Sinha,

who have worked on various aspects of the work reported here. Work at Argonne is supported by the DOE-Basic Energy Sciences under W-31-109-ENG-38.

References

[1] M.B. Maple, Physica B 215 (1995) 110.
[2] J.W. Lynn, S. Skanthakumar, Q. Huang, S.K. Sinha, Z. Hossain, L.C. Gupta, R. Nagarajan, C. Godart, Phys. Rev. B 55 (1997) 6584 , and references therein.
[3] T.E. Grigereit, J.W. Lynn, Q. Huang, A. Santoro, R.J. Cava, J.J. Krajewski, J.W.F. Peck, Phys. Rev. Lett. 73 (1994) 2756.
[4] A.I. Goldman, C. Stassis, P.C. Canfield, J. Zarestky, P. Dervenagas, B.K. Cho, D.C. Johnston, B. Sternlieb, Phys. Rev. B (1994) R9668.
[5] P. Dervenagas, J. Zarestky, C. Stassis, A.I. Goldman, P.C. Canfield, B.K. Cho, Phys. Rev. B 53 (1996) 8506.
[6] L.J. Chang, C.V. Tomy, D.M. Paul, C. Ritter, Phys. Rev. B 54 (1996) 9031.
[7] A. Kreyssig, M. Lowenhaupt, K.-H. Muller, H.G. Fuchs, A. Handstein, C. Ritter, Physica B 234 (1997) 737.
[8] T. Siegrist, H.W. Zandbergen, R.J. Cava, J.J. Krajewski, J.W.F. Peck, Nature 367 (1994) 254.
[9] C. Detlefs, A.H.M.Z. Islam, A.I. Goldman, C. Stassis, P.C. Canfield, J.P. Hill, D. Gibbs, Phys. Rev. B 55 (1997) R680.
[10] C. Detlefs, A.I. Goldman, C. Stassis, P.C. Canfield, B.K. Cho, J.P. Hill, D. Gibbs, Phys. Rev. B 53 (1996) 6355.
[11] E. Alleno, Z. Hossain, C. Godart, R. Nagarajan, L.C. Gupta, Phys. Rev. B 52 (1995) 7428.
[12] S.K. Dhar, R. Nagarajan, Z. Hossain, C. Godart, L.C. Gupta, R. Vijayaraghavan, Solid State Commun. 98 (1996) 985.
[13] Z. Hossain, R. Nagarajan, R. Pattalwar, S.K. Dhar, L.C. Gupta, C. Godart, Physica B 230–232 (1997) 865.
[14] A. Yatskar, N.K. Budraa, W.P. Beyermann, P.C. Canfield, S.L. Budko, Phys. Rev. B 54 (1996) 3772.
[15] P.C. Canfield, S.L. Bud'ko, J. Alloys Compounds 262–263 (1997) 169.
[16] Z.Q. Peng, K. Krug, K. Winzer, Phys. Rev. B 57 (1998) 8123.
[17] H. Eisaki, H. Takagi, R.J. Cava, K. Mizuhashi, J.O. Lee, B. Batlogg, J.J. Krajewski, J.W.F. Peck, S. Uchida, Phys. Rev. B 50 (1994) 647.
[18] C. Detlefs, A.H.M.Z. Islam, T. Gu, A.I. Goldman, C. Stassis, P.C. Canfield, J.P. Hill, T. Vogt, Phys. Rev. B 56 (1997) 7843.
[19] Y. Rhee, X. Wang, B.N. Harmon, Phys. Rev. B 51 (1995) 15585.
[20] A. Amici, P. Thalmeier, Phys. Rev. B 57 (1998) 10864.
[21] Q. Huang, J.W. Lynn, A. Santoro, B.C. Chakoumakos, R.J. Cava, J.J. Krajewski, J.W.F. Peck, Physica C 271 (1996) 311.
[22] L.J. Chang, C.V. Tomy, D.M. Paul, N.H. Andersen, M. Yethiraj, J. Phys.: Condens. Matter 8 (1996) 2119.
[23] F. Bourdarot, J.W. Lynn, Q. Huang, D.R. Sanchez, M.B. Fontes, J.C. Trochez, E. Baggio-Saitovitch, preprint
[24] J.C. Trochez, D.R. Sanchez, B. Giordanengo, M.B. Tontes, M. Continentino, E.M. Baggio-Saitovitch, Physica C 282–287 (1997) 1939.